Control of a Gantry Crane using Input Shaping Schemes with Distributed Delay

Mohammad Javad Maghsoudi[1], Z. Mohamed[1]*, M.O. Tokhi[2], A.R. Husain[1] and M.S. Z. Abidin[1]

[1]Faculty of Electrical Engineering, Universiti Teknologi Malaysia, 81310 UTM Johor Bahru, Johor, Malaysia

[2]Department of Automatic Control and Systems Engineering, The University of Sheffield, UK

*Corresponding Author:
 E-mail address: zahar@fke.utm.my, Tel: +607-5557019, Fax: +607-5566272

Abstract

This paper presents simulation and real-time implementation of input shaping schemes with a distributed delay for control of a gantry crane. Both open-loop and closed-loop input shaping schemes are considered. Zero Vibration and Zero Vibration Derivative input shapers are designed for performance comparison in terms of trolley position response and level of sway reduction. Simulation and experimental results have shown that all the shapers are able to reduce payload sway significantly while maintaining satisfactory position response. Investigations with different cable lengths that correspond to ±20% changes in the sway frequency have shown the distributed delay-based shaper has asymmetric robustness behavior. The shaper provides highest robustness for the case of 20% increase in the sway frequency but lower robustness for the case of 20% decrease. However, other schemes give symmetric robustness behavior for both cases.

Keywords:

Distributed delay shaper; Input shaping; Gantry crane; Robustness; Sway reduction

1. Introduction

Input shaping is one of the most useful approaches to reduce motion-induced oscillations of oscillatory systems (Singhose, 2009). The input shaping theory was introduced in the late 1950's (Smith, 1957) and the well-known input shaping technique was introduced by Singer and Seering (1990). Researchers have utilized different types of input shapers including Zero Vibration (ZV) and Zero Vibration Derivative (ZVD) (Mohamed et al., 2005), negative shapers (Singhose et al., 1994), multi-hump extra intensive shapers (Singhose et al., 1996), two mode shapers (Crain et al., 1996), adaptive shapers (Pereira et al., 2012) and unity magnitude shapers (Pao and Singhose, 1996; Gürleyük, 2011)). The input shaping has been implemented on a real gantry crane (Singer et al., 1997) and has been proven to be successful in reducing payload

sway during hoisting. Recently, implementing methods of input shaping for control of vibration have been improved by researchers (Yang et al., 2014).

A gantry crane is one of the mostly used industrial crane in industries, factories and ware houses (Butler et al., 1991). Shipping yards and nuclear facilities are the other places where heavy loads must be transferred by gantry cranes. One of the significant factors affecting productivity and efficiency of the industrial systems is speed. However, it is obvious for a gantry crane, fast manoeuvres resulted in significant payload oscillation and considerable residual sway and negatively affects performance of the systems (Sorensen et al., 2007; Yu et al., 2014). At higher speeds, these sway angles prevent the payload to settle down during movement and unloading. This problem will be crucial particularly for industrial applications where operators should manipulate the cranes (Peng et al., 2012). Vast applications of cranes have encouraged many researchers to reduce the motion-induced oscillation of these structures (Le et al., 2014).

Recently, a new input shaping scheme has been proposed based on a distributed delay (Vyhlídal et al., 2013) known as Distributed Zero Vibration (DZV) shaper, whereas other input shapers have been developed based on a lump type delay. However, its application for control of flexible systems such as gantry crane has not been investigated. This paper presents simulation and experimental study on the implementation of DZV shaper for control of a gantry crane both in open-loop and closed-loop input shaping schemes. Comparisons with ZV and ZVD shapers are provided to examine the performance of the DZV shaper. Initially, a complete mathematical model of the system is obtained based on Newtonian techniques. Curve fitting box of Matlab is utilized to find natural frequency and damping ratio of the system based on the sway output of the actual crane. For the closed-loop system, a closed-loop input shaping with PID controller is designed by considering saturation and dead band of the real crane system. Finally, the robustness performance of the control schemes to uncertainty in the cable length that changes the natural frequency of the crane is examined.

2. Gantry Crane Dynamic

Figure 1 shows a lab-scaled gantry crane used in this study. The gantry crane is capable of transferring a load from any location to a desired place in a restricted three dimensional space. The length, height and width of the crane are 1.0 m. The system hardware consists of three main components: a cart, a rail and a pendulum. Three DC 24 V motors are used to move the cart, rail and payload. These motors are actuated by specific DC drivers that produce corresponding sequence of PWM pulses. Both cart and rail are capable of moving in X direction but only cart is able to move in Y direction. The payload is lowered and lifted in Z direction. Therefore, the payload can move freely in three directions. The mathematical model is obtained based on the given characteristics of the crane by the manufacturer and the study by Pauluk *et al.* (2001). The obtained model is simulated using Simulink to investigate dynamic behaviour of the system.
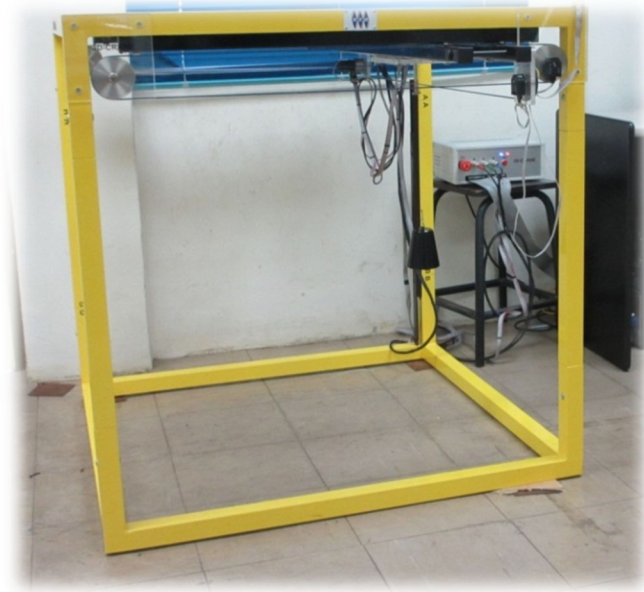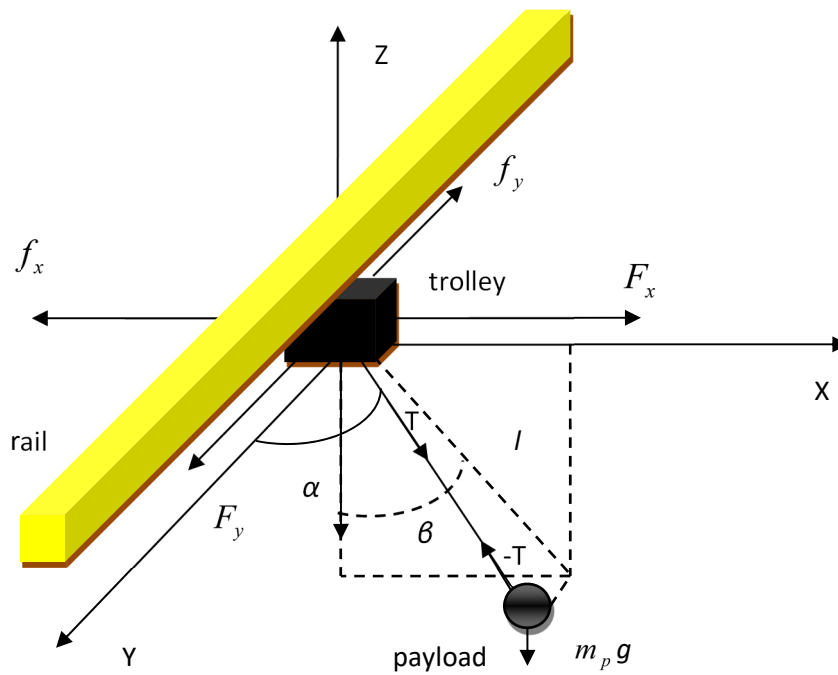
Figure 1. A lab-scaled 3D gantry crane

Figure 2. Schematic diagram and forces

A schematic diagram of the 3D gantry crane system is shown in Figure 2 with *XYZ* as the coordinate system. m_p, m_t and m_r are the payload mass, trolley mass (including gear box, encoders and DC motor) and moving rail respectively. *l* represents the length of the lift-line, *α* represents the angle of lift-line with *Y* axis and *β* represents angle between negative part of *Z* axis and projection of the payload cable onto the *XZ* plane. *T* is a reaction force in the payload cable acting on the trolley, F_x and F_y are the forces driving the rail and trolley respectively, F_z is a force lifting the payload and f_x, f_y and f_z are corresponding friction forces. By defining

$$\mu_1 = \frac{m_p}{m_t}, \mu_2 = \frac{m_p}{m_t + m_r}; \quad u_1 = \frac{F_x}{m_t}, u_2 = \frac{F_y}{m_t + m_r}, u_3 = \frac{F_z}{m_p}; \quad f_1 = \frac{f_x}{m_t}, f_2 = \frac{f_y}{m_t + m_r}, f_3 = \frac{f_z}{m_p}$$

$$K_1 = u_1 - f_1, K_2 = u_2 - f_2, K_3 = u_3 - f_3$$

the dynamic equations of motion of the crane can be obtained as (Pauluk et al., 2001)

$$\ddot{x}_t = K_2 + \mu_2 K_3 \sin\alpha \sin\beta \tag{1}$$

$$\ddot{y}_t = K_1 + \mu_1 K_3 \cos\alpha \tag{2}$$

$$\begin{aligned}\ddot{x}_p = \ddot{x}_t + (\ddot{l} - l\dot{\alpha}^2 - l\dot{\beta}^2)\sin\alpha\sin\beta + 2l\dot{\alpha}\dot{\beta}\cos\alpha\cos\beta \\ + (2\dot{l}\dot{\alpha} + l\ddot{\alpha})\cos\alpha\sin\beta + (2\dot{l}\dot{\beta} + l\ddot{\beta})\sin\alpha\cos\beta\end{aligned} \tag{3}$$

$$\ddot{y}_p = \ddot{y}_t + (\ddot{l} - l\dot{\alpha}^2)\cos\alpha - (2\dot{l}\dot{\alpha} + l\ddot{\alpha})\sin\alpha \tag{4}$$

$$\begin{aligned}\ddot{z}_p = (-\ddot{l} + l\dot{\alpha}^2 + l\dot{\beta}^2)\sin\alpha\cos\beta + 2l\dot{\alpha}\dot{\beta}\cos\alpha\sin\beta \\ - (2\dot{l}\dot{\alpha} + l\ddot{\alpha})\cos\alpha\cos\beta + (2\dot{l}\dot{\beta} + l\ddot{\beta})\sin\alpha\sin\beta\end{aligned} \tag{5}$$

where x_p, y_p and z_p are position of payload in *X*, *Y* and *Z* axes respectively. x_t and y_t are positions of trolley in *X* and *Y* axes. Dots represent derivative of the respective quantities. Although the obtained model considers a 3D gantry crane, the rail movement is not considered in this study to shorten the paper. It is envisaged that similar results are achieved for trolley and rail movements. Table 1 shows the parameters used for simulation and experiment which correspond to the lab-scaled crane shown in Figure 1.

Table 1. System parameters

Variables	Values
Mass of payload, m_p	1 kg
Mass of trolley, m_t	1.155 kg
Mass of moving rail, m_r	2.2 kg
Cable length, l	0.47 m
Gravitational constant, g	9.8 m/s
Corresponding friction forces, f_x, f_y, f_z	100, 82, 75 Ns/m

3. Control Schemes

A brief description and derivation of the control techniques is presented in this section. These include the open loop control scheme based on input shaping techniques and feedback control scheme utilising PID controller. The 3D gantry crane system under consideration is a nonlinear system and designing controllers normally involves linearisation and simplification of the equations (Sorensen et al., 2007). For this reason, in some special operating points there would be a slight difference between the performance of real and modeled systems (Abdel-Rahman et al., 2003). For instance, input shaping scheme is able to eliminate completely the residual sway of a simple second order crane model whereas there would be a slight residual sway in the sway response of the real crane. In this study, the nonlinear model is implemented and utilised for simulation. For this purpose, optimisation based tuning is utilised to tune the PID controllers for the gantry crane system.

3.1. ZV and ZVD Shapers

Input shaping is a feed-forward control technique that involves filtering a desired command with an input shaper. A mathematical description of a general input shaper may be expressed as

$$IS(t) = \sum_{j=1}^{m} A_j \delta(t - t_j) \tag{6}$$

where $\delta(t)$ represents the Dirac delta function, t_j is time of a jth pulse and a non-negative value and A_j is amplitude of jth pulse and a non-zero value. The shaped input that results from the convolution will drive the system and the shaped command reduces the detrimental effects of the oscillatory system. An oscillatory system can be modeled as a superposition of second order systems each with a transfer function

$$G(s) = \frac{\omega_n^2}{s^2 + 2\zeta\omega_n s + \omega_n^2} \tag{7}$$

where ω_n is the natural frequency and ζ is the damping ratio of the system. Thus, the impulse response of a single mode system at time t is

$$y(t) = \frac{A\omega_n}{\sqrt{1-\zeta^2}} e^{-\zeta\omega_n(t-t_o)} \sin(\omega_n\sqrt{1-\zeta^2}(t-t_o)) \qquad (8)$$

where A and t_0 are the amplitude and time of the impulse respectively. Further, the response to a sequence of impulses can be obtained using the superposition principle. For m impulses, with $\omega_d = \omega_n\sqrt{1-\zeta^2}$, the impulse response can be expressed as

$$y(t) = M\sin(\omega_d t + \alpha_1) \qquad (9)$$

where, $\quad M = \sqrt{(\sum_{j=1}^{m} B_j\cos\phi_j)^2 + (\sum_{j=1}^{m} B_j\sin\phi_j)^2}$, $\quad B_j = \frac{A_j\omega_n}{\sqrt{1-\zeta^2}} e^{-\zeta\omega(t-t_j)}$, $\quad \phi_j = \omega_d t_j \quad$ and

$\alpha_1 = \tan^{-1}\left(\sum_{j=1}^{m} \frac{B_j\cos\phi_j}{B_j\sin\phi_j}\right)$. A_j and t_j are the magnitudes and times at which the impulses occur.

The residual single mode vibration amplitude of the impulse response is obtained at the time of the last impulse, t_m as

$$V = \sqrt{V_1^2 + V_2^2} \qquad (10)$$

where $V_1 = \sum_{j=1}^{m} \frac{A_j\omega_n}{\sqrt{1-\zeta^2}} e^{-\zeta\omega_n(t_m-t_j)}\cos(\omega_d t_j)$, $V_2 = \sum_{j=1}^{m} \frac{A_j\omega_n}{\sqrt{1-\zeta^2}} e^{-\zeta\omega_n(t_m-t_i)}\sin(\omega_d t_j)$.

To achieve zero vibration after the last impulse, it is required that both V_1 and V_2 in Equation (10) are independently zero. Furthermore, to ensure that the shaped command input produces the same rigid body motion as the unshaped command, it is required that the sum of amplitudes of the impulses is unity. To avoid response delay, the first impulse is selected at time $t_1 = 0$. Hence by setting V_1 and V_2 in Equation (10) to zero, $\sum_{j=1}^{m} A_j = 1$ and solving yields a two-impulse sequence with parameters as (Singer and Seering, 1990)

$$t_1 = 0, \quad t_2 = \frac{\pi}{\omega_d},$$

$$A_1 = \frac{1}{1+K}, \quad A_2 = \frac{K}{1+K}. \qquad (11)$$

where $K = e^{-\frac{\zeta\pi}{\sqrt{1-\zeta^2}}}$. This is known as ZV shaper. Figure 3 shows the designing process of a shaped input using a ZV shaper.
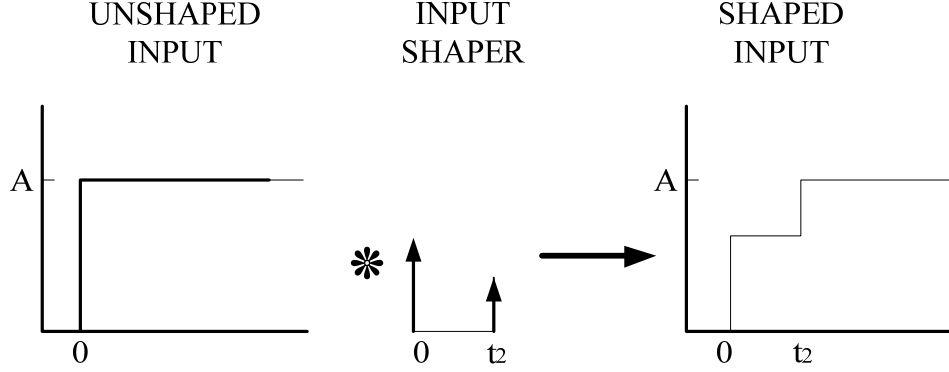
Figure 3: ZV input shaping

The robustness of the input shaper to errors in natural frequencies of the system can be increased by setting $dV/d\omega_n = 0$. Setting the derivative to zero is equivalent of producing small changes in vibration corresponding to natural frequency changes. By obtaining the first derivatives of V_1 and V_2 in Equation (10) and simplifying, yields a three-impulse sequence with parameters as

$$t_1 = 0, \quad t_2 = \frac{\pi}{\omega_d}, \quad t_3 = \frac{2\pi}{\omega_d},$$

$$A_1 = \frac{1}{1+2K+K^2}, \quad A_2 = \frac{2K}{1+2K+K^2}, \quad A_3 = \frac{K^2}{1+2K+K^2} \qquad (12)$$

where K is as in Equation (11). This is known as ZVD shaper.

3.2. DZV Shaper

The input shaping needs dividing the input signal into some different signals with a specific delay. In the ZV and ZVD shapers, the delay is a lumped type delay. However, in the recently proposed DZV shaper (Vyhlídal et al., 2013), the delay is distributed. Both types of delay can be described as

$$y(t) = \int_0^{\beta} x(t-\varepsilon)dw(\varepsilon) \qquad (13)$$

where y and x are the delay output and input respectively. The delay distribution over the interval $[0, \beta]$ is described by $w(\varepsilon)$ where β is the upper limit. The equally distributed delay as shown in Figure 4 can be formulated as

$$w(\varepsilon) = \begin{cases} 0, & \varepsilon < 0 \\ \dfrac{1}{\beta}\varepsilon, & \varepsilon \in [0,\beta] \\ 1, & \varepsilon > \beta \end{cases} \qquad (14)$$
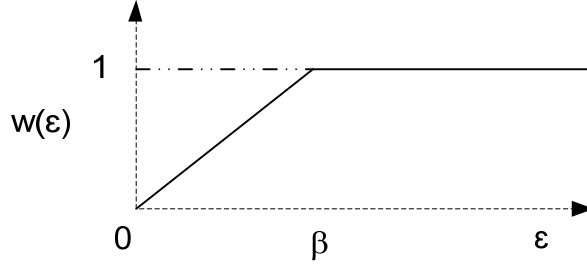

Figure 4: The equally distributed delay

As $dw(\varepsilon) = \dfrac{1}{\beta}d\varepsilon$ for $\varepsilon \in [0,\beta]$, Equation (13) can be written as

$$y(t) = \frac{1}{\beta}\int_0^\beta x(t-\varepsilon)d\varepsilon \qquad (15)$$

Using Laplace transform with zero initial conditions, the DZV transfer function can be described as

$$D(s,\beta) = \frac{1-e^{-s\beta}}{s\beta} \qquad (16)$$

The DZV shaping process is illustrated in Figure 5 and a new shaped input is obtained which is different from the ZV and ZVD type shaped inputs. For a second order oscillatory system as formulated in Equation (7), the values of D and β can be obtained as (Vyhlídal et al., 2013)

$$\omega_n e^{-\xi\beta} + \xi\sin(\omega_n\beta) - \omega_n\cos(\omega_n\beta) = 0 \qquad (17)$$

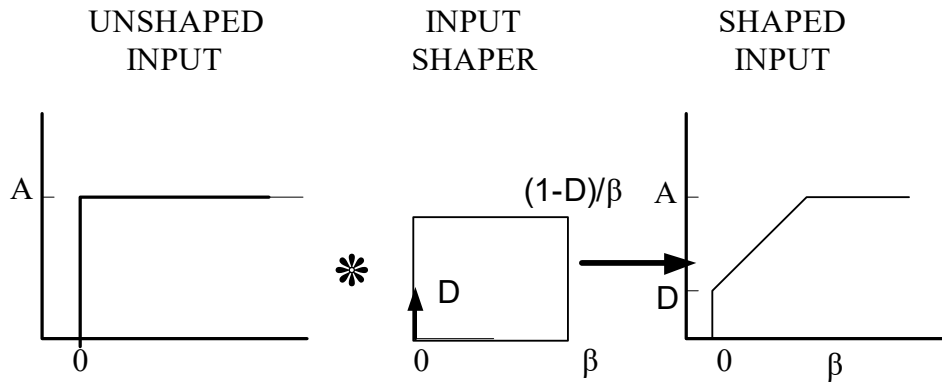$$D = \frac{\sin(\omega_n\beta)}{\sin(\omega_n\beta) - \beta\omega_n e^{-\xi\beta}} \qquad (18)$$

8

UNSHAPED
INPUT

INPUT
SHAPER

SHAPED
INPUT

Figure 5: DZV Shaper

3.3. Open loop Control

Open loop control scheme is utilised in several industrial applications to transfer loads using gantry cranes. Therefore, it is desirable to study the performance of input shapers based on lumped-based delay (ZV and ZVD) and distributed-based delay (DZV) in reducing the payload sway in an open loop configuration. Figure 6 shows the feed-forward input shaping technique used for position control of the trolley where x and θ represents trolley position and payload sway angle respectively.
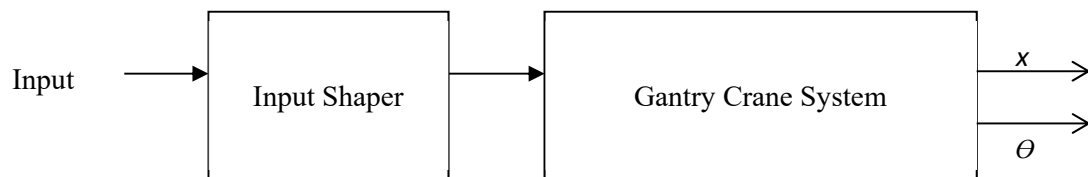
Figure 6: Open loop control scheme with input shaping

3.4. Closed-Loop Input Shaping Control

To further investigate the performance of DZV shaper, closed-loop input shaping scheme with PID controller is designed. Figure 7 shows a block diagram of the system where $xref$ and x represent desired and actual positions of the trolley respectively. In this study, a PID feedback control of collocated sensor signals is adopted for control of trolley motion of the crane where the PID controller block consists of the proportional gain (K_p), integrator gain (K_i) and derivative gain (K_d). The PID controllers are designed independently for three different shapers. Essentially, the task of this controller is to position the trolley to a specified position of demand without payload's sway consideration. The position signals are fed back and used to control the position of the trolley. As the input voltage of the lab-scaled gantry crane is limited and higher voltage may damage the DC motors of the crane, a saturation block is considered to limit the input voltage to the system. It is found that inputs with the values lower than 10% of the maximum value cannot actuate the motors while these inputs can affect the output of simulation block. For this reason a dead-zone block is added into the Simulink model

to ensure accurate simulation results. For comparison, ZV and ZVD shapers are also designed for the closed-loop system.
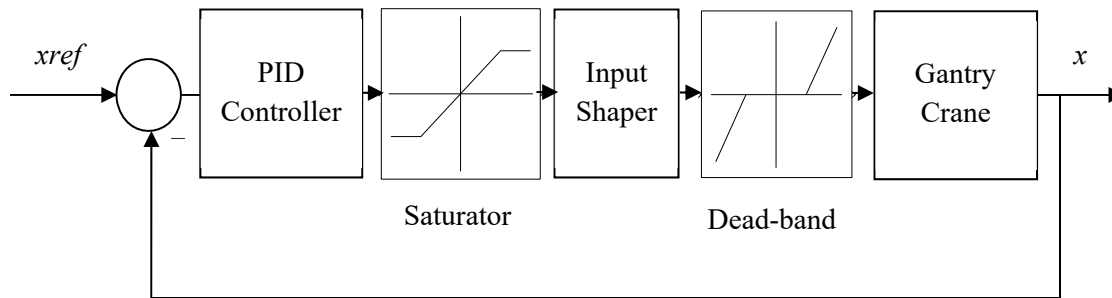

Figure 7: Closed loop input shaping control scheme with PID controller

4.   Simulation Results

In this section, the shapers are implemented and tested within the simulation environment of the gantry crane system. The simplest shaper to be implemented is ZV shaper as it needs only gain and delay elements. ZVD shaper is similar to ZV shaper with only one additional delay element. However, DZV needs gain, delay and integrator elements and can be considered as the most difficult shaper to be implemented. Simulink is used to implement the open loop and closed loop control schemes. Natural frequency and damping ratio of the lab-scaled gantry crane are obtained as $\omega_n = 4.57$ Hz and $\zeta = 0.008$. Subsequently, the three shapers are designed using Equations (11), (12), (17) and (18) and the calculated parameters of the shapers are given in Table 2. The ZV, ZVD and DZV shapers are simulated based on the obtained values.

Table 2: Parameters of the shapers

ZV				ZVD						DZV	
A_1	A_2	t_1	t_2	A_1	A_2	A_3	t_1	t_2	t_3	D	β
0.506	0.494	0	0.688	0.256	0.499	0.244	0	0.688	1.375	0.052	1.306

4.1. Open-Loop Control

Figure 8 shows the unshaped and three shaped torque inputs applied to the gantry crane system. It can be shown that ZV and ZVD shaped signals have the shortest and longest delay respectively while DZV shaped signal delay is located in between the others. Figure 9 shows the sway response of the payload for all input torques. Input shaping has significantly reduced the residual sway of the payload from 3.65 degrees to about 0.8 degrees. The reason that input shaping has not completely eliminated the residual sway is that the nonlinear model is implemented for simulation rather than the simple second order model similar to Equation (7).

Considering zero as desired sway, Integrated Absolute Error (IAE) values for unshaped, ZV, ZVD and DZV are 1025, 251, 262 and 241 respectively. A low IAE value is desirable as this indicates low sway. All the shapers reduce the IAE to nearly one-fourth of the unshaped value. It is also noted that sway response of payload using DZV shaper has the lowest transient sway, about 1.32 degrees. The fastest and slowest response are obtained using ZV technique (0.688 s) and ZVD technique (1.375 s) respectively.
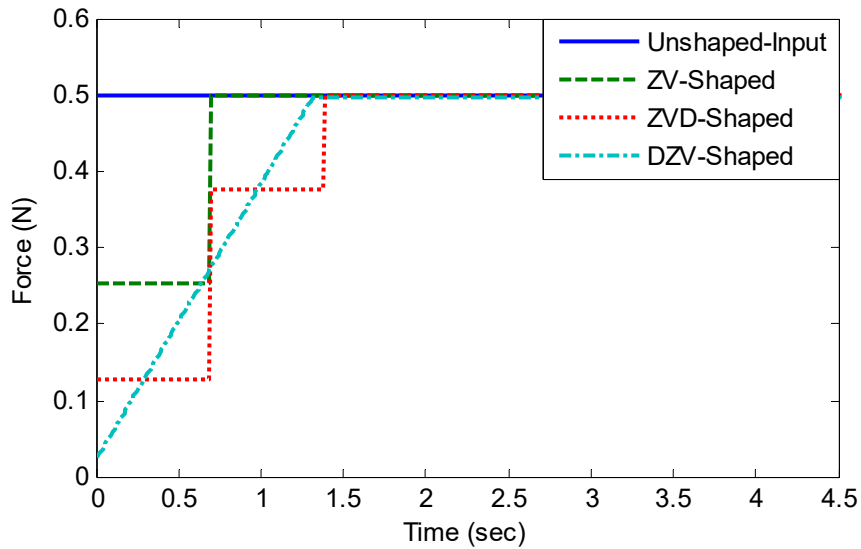
Figure 8: Input to the open loop systems (simulation)
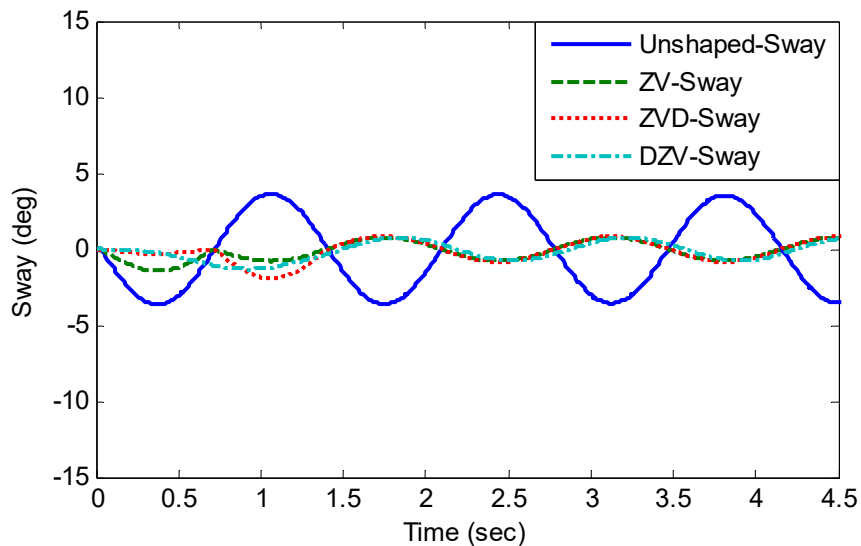
Figure 9: Sway of the payload for the open loop systems (simulation)

4.2. Closed-Loop Control

The PID gains for all control schemes are shown in Table 3 and the shapers' parameters as in Table 2. The closed-loop input shaping system with PID controller shown in Figure 7 is

11

simulated without input shaper (unshaped) and with the three shapers (ZV, ZVD and DZV). The gantry crane is required to move to a desired location of 0.55 m.

Simulation results of trolley control signal shown in Figure 10 indicate that ZV shaped system produces the lowest delay as compared to other shaper systems. The position responses of all control schemes are shown in Figures 11. It is noted with the PID gains, the desired trolley location is achieved without overshoot using all the control schemes. Table 4 summarises the settling time of the position responses using all shapers, where ZV provides the fastest response with 2.31 s follows by DZV and ZVD.

Table 3: Controller gains for different closed loop systems

Unshaped			ZV-Shaped			ZVD-Shaped			DZV-Shaped		
K_p	K_i	K_d	K_p	K_i	K_d	K_p	K_i	K_d	K_p	K_i	K_d
14.8	0.03	-1.84	6.33	-0.12	0.37	3.6	-0.08	0.55	4.89	-0.1	1.12

Table 4: Settling time and IAE values of system responses (simulation)

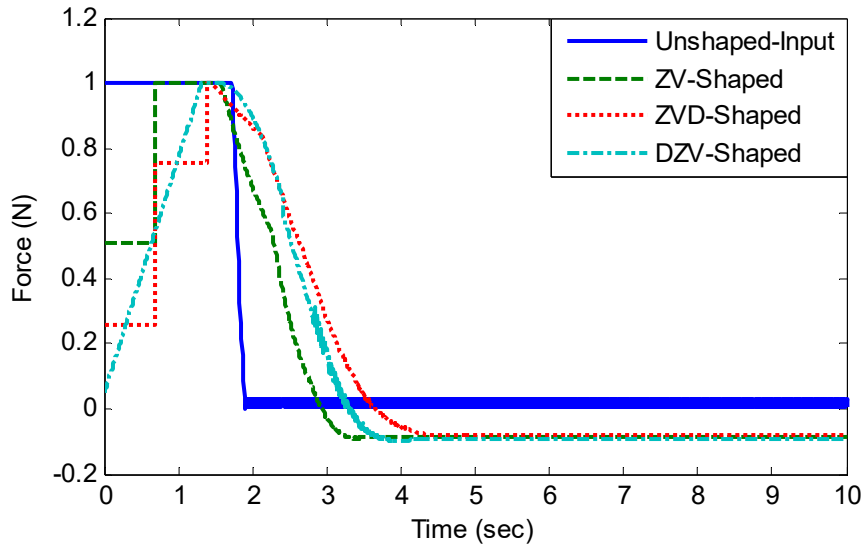| Control scheme	Settling time (s)	IAE (Sway)
Unshaped	1.73	7421
ZV	2.31	859
ZVD	2.83	1057
DZV	2.64	1314

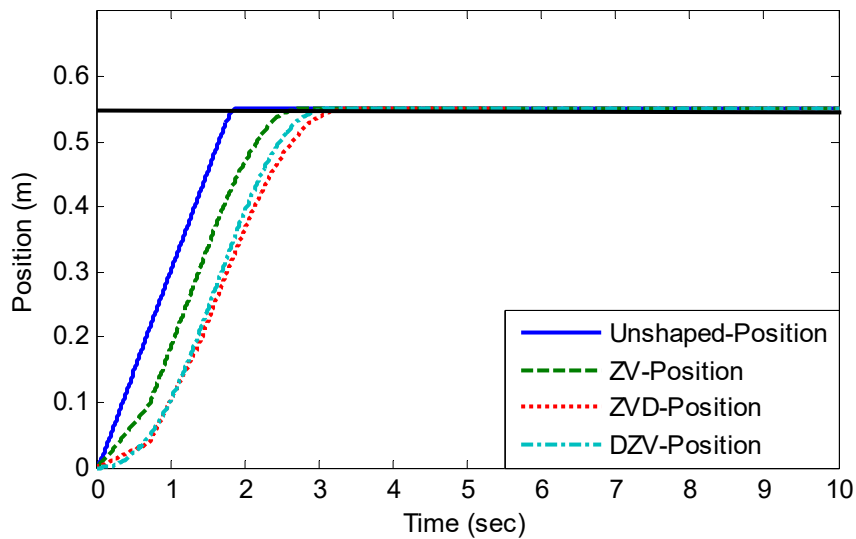Figure 10: Control signals of the closed loop systems (simulation)

Figure 11: Position of trolley for the closed loop systems (simulation)

Figures 12 show the payload sway response for all control schemes. The results show that all the shapers are able to reduce the residual sway significantly from 12.8 degrees to about 2 degrees. DZV shaper provides the lowest transient sway (2.84 degrees) but has the highest residual sway (2.08 degrees) whereas ZV shaper provides the lowest residual sway (1.04 degrees) and highest transient sway (3.7 degrees). IAE values for unshaped, ZV, ZVD and DZV are 7421, 859, 1057 and 1314 respectively. This is the advantage of using input shapers although a slight delay in the position response occurs.
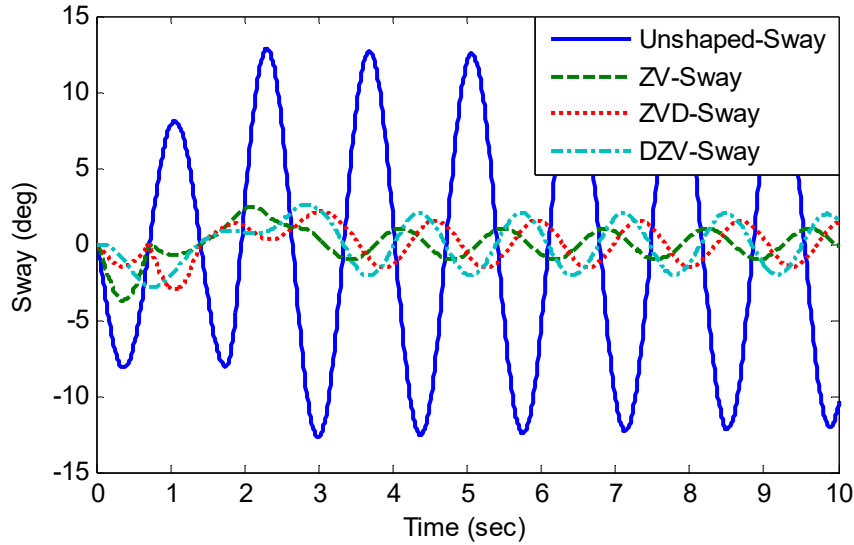
Figure 12: Sway of payload for the closed loop systems (simulation)

4.3. Robustness

For evaluation of robustness of the control schemes, the crane system with different cable lengths is considered. In this case, $l = 0.326$ m and $l = 0.73$ m are used with payload sway frequency of 5.49 Hz and 3.66 Hz respectively. These imply $\pm 20\%$ error in the sway frequency as compared to the first case with $l = 0.47$ m. Figures 13 and 14 show simulation responses to a step input in the open-loop configuration for $l = 0.326$ m and $l = 0.73$ m respectively.
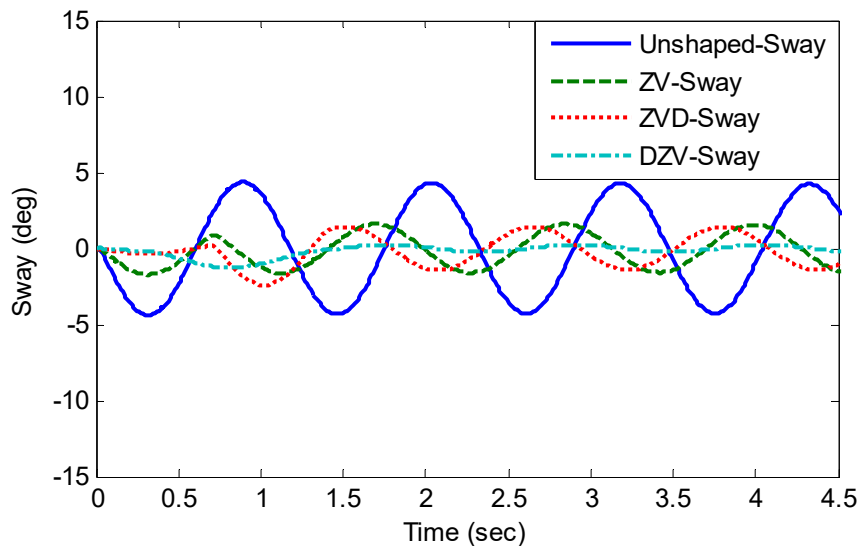
Figure 13: Sway of payload with 20% increase in natural frequency (simulation)

14
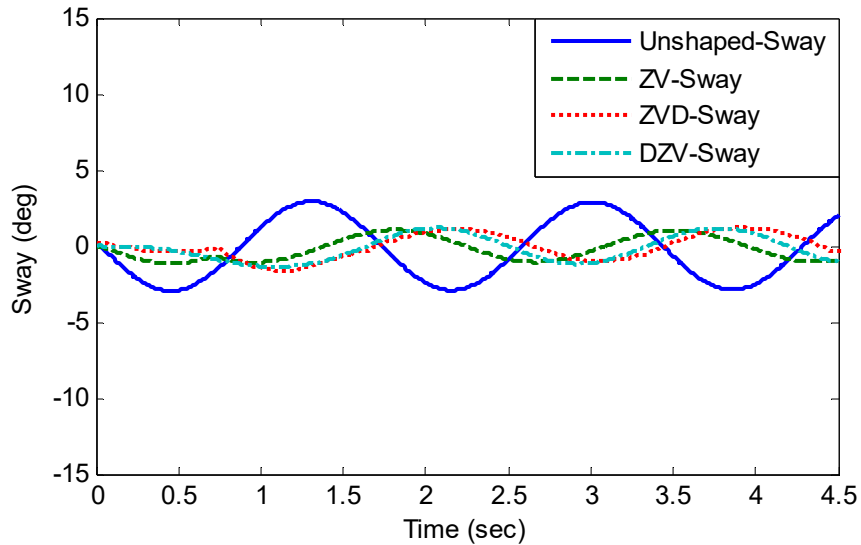
Figure 14: Sway of payload with 20% decrease in natural frequency (simulation)

The results show that within ±20% error tolerance, all the shapers are able to reduce the payload sway at least by half of the response with unshaped input. The IAE values and maximum residual sway for both cases using unshaped input, and ZV, ZVD and DZV shapers are summarised in bar charts in Figures 15 and 16 respectively. Further investigations noted that DZV shaper has an asymmetric behavior in respond to uncertainties in the natural frequency. Significant differences in the shaper's performance can be seen in both bar charts. With 20% increase in the natural frequency, DZV is found to have highest robustness performance with lowest IAE value and maximum residual sway. However as the natural frequency reduce by 20%, robustness performance of DZV decreases which is almost similar to ZV shaper. On the other hand, ZV and ZVD shapers show similar behavior for both +20% and -20% errors in the natural frequency. As expected, ZVD shaper shows higher robustness than ZV shaper.
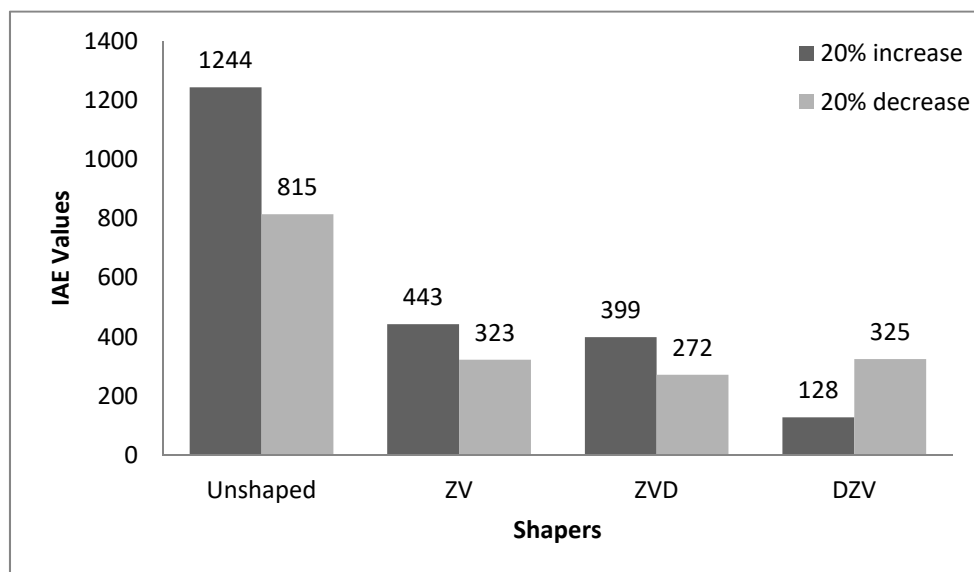

Figure 15: IAE values of the payload sway for 20% increase and decrease in the natural frequency
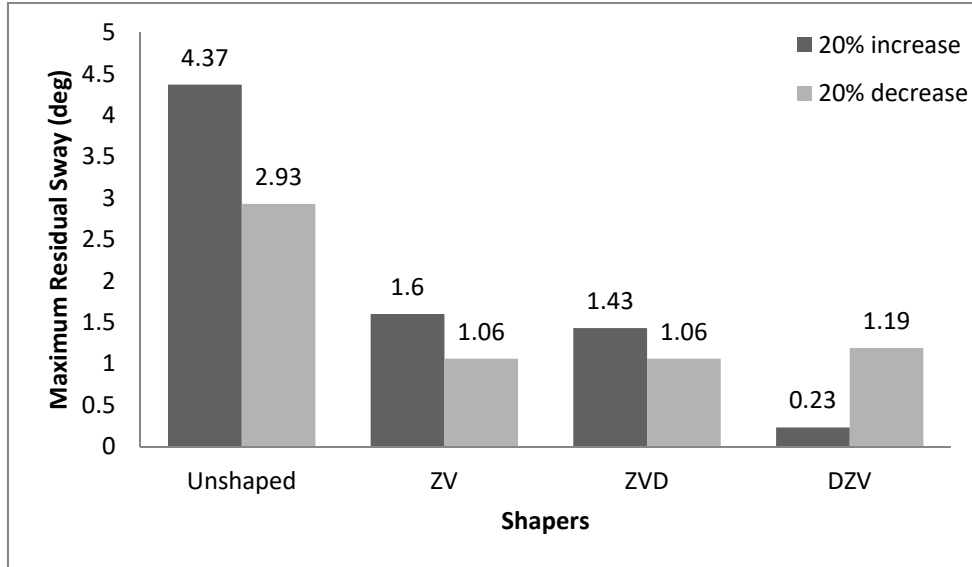
15

Figure 16: Maximum residual sway for 20% increase and 20% decrease in the natural frequency

5.   Experimental Results

Experiments were performed on a lab-scaled gantry crane shown in Figure 1 to validate the simulation results. The crane is equipped with 5 incremental encoders to measure the position of trolley in X and Y directions (only X is considered in this paper), position of payload in Z direction and the payload sway in X and Y directions. All the data are transmitted on-line to a PC by an interface card. The motors are also actuated by specific DC drives. Similar input as used for simulation is applied to the real gantry crane.

5.1. Open-Loop Control

Figure 17 shows the sway response of the payload to similar inputs as in the simulation (Figure 8). The results verify the simulation results where the input shaping has reduced significantly the motion induced sway of the payload. The residual sway of the payload has been reduced from 4 degrees to about 0.8 degrees. The IAE values for unshaped, ZV, ZVD and DZV are 1007, 269, 188 and 200 respectively. This verifies the simulation results where IAE values for shaped inputs are nearly one-fourth of the IAE of unshaped input. Similar to the simulation results, sway response of payload utilizing DZV shaper has the lowest transient sway (1.4 degrees).
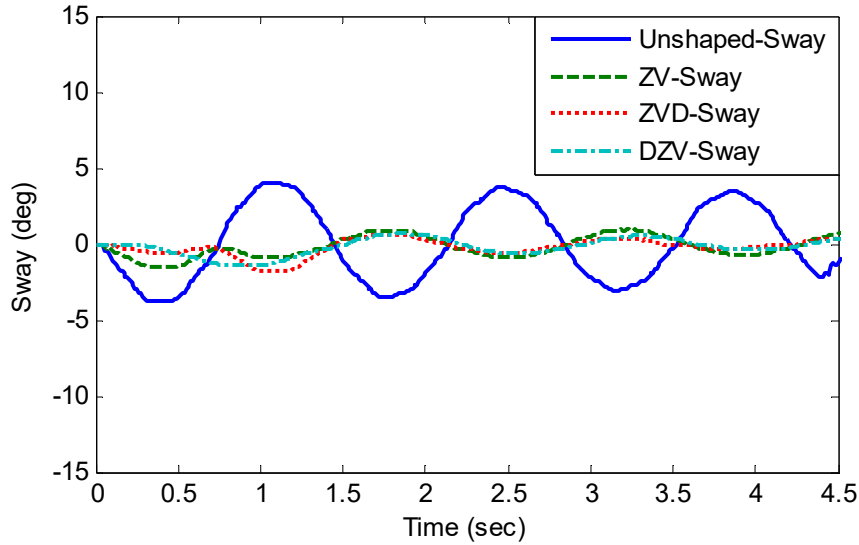
Figure 17: Sway of the payload for the open loop systems (experiment)

5.2. Closed-Loop Control

Similar PID gains and input shapers' parameters as in the simulation (Tables 2 and 3) are used for experiment. Experimental control signal for trolley in Figure 18 verify that ZV shaped system produces less delay compared to other shaper systems. The experimental position responses of the control schemes systems are shown in Figure 19 and Table 5 summarises the settling time and overshoot of the position responses. It is noted that the position responses show no overshoot for unshaped signal while overshoots of ZV, ZVD and DZV increase to 1.89%, 3.03% and 5.05% respectively. For the settling time, similar pattern as the simulation result is obtained where ZV gives the fastest response and ZVD is the slowest.

Table 5: Settling time, overshoot and IAE values of system responses (experiment)

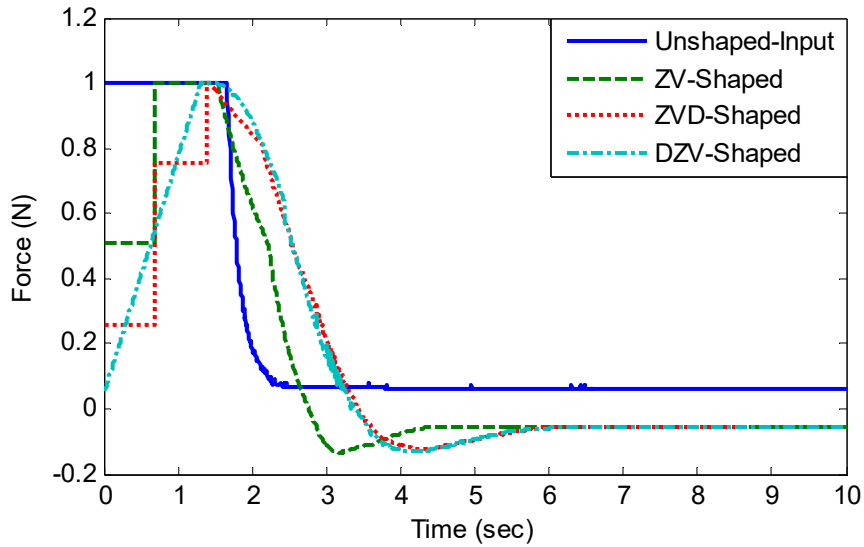| Control Scheme	Settling time (s)	Overshoot (%)	IAE (Sway)
Unshaped	1.73	0	5911
ZV	2.2	1.89	1005
ZVD	2.65	3.03	1066
DZV	2.56	5.05	1108

Figure 18: Control signals of the closed loop systems (experiment)

Figure 20 shows the payload sway response using the control schemes. The results verify the simulation where the three shapers reduce motion induced sway significantly from 9.84 degrees to about 1.5 degrees. The IAE values are obtained as 5911, 1005, 1066 and 1108 for the unshaped, ZV, ZVD and DZV shapers respectively. Similar to the simulation results, ZV shaper provides the lowest residual sway (1.4 degrees) and the highest transient sway (3.6 degrees), while DZV shaper provides the lowest transient sway (2.7 degrees) and the highest residual sway (1.8 degrees).
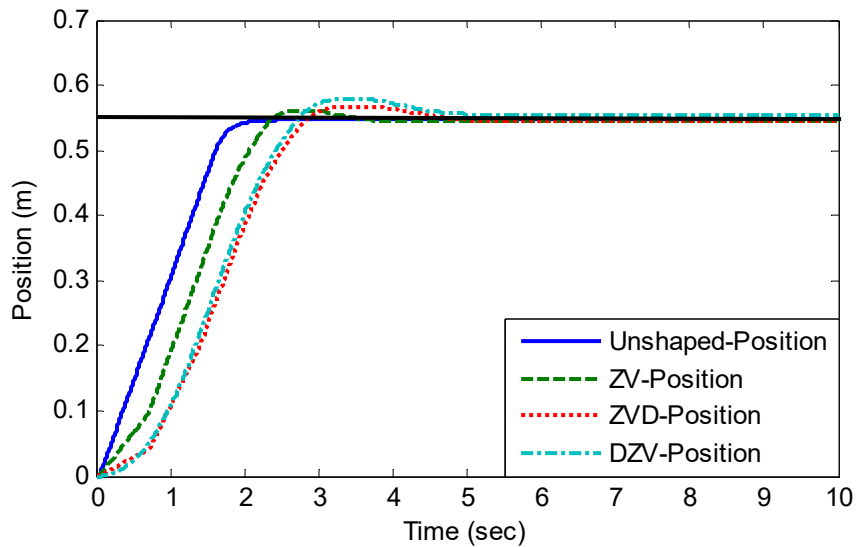

Figure 19: Position of trolley for the closed loop systems (experiment)
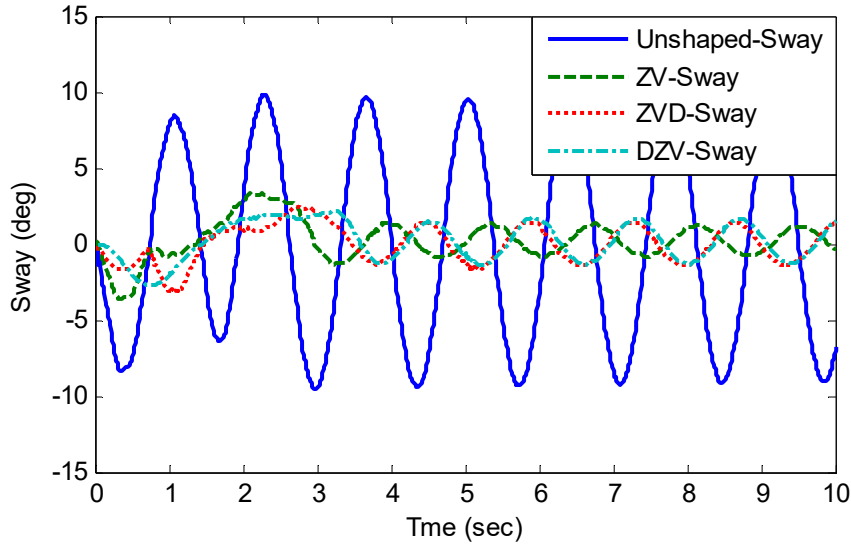
Figure 20: Sway of payload for the closed-loop systems (experiment)

5.3. Robustness

Similar to the simulation study, the crane system with ±20% error in sway frequencies is used for robustness analysis. Thus, sway frequencies of 5.49 Hz and 3.66 Hz that corresponds to $l = 0.326$ m and $l = 0.73$ m respectively are considered and experiments are performed on the real lab-scaled gantry crane with new cable lengths. Figures 21 and 22 show experimental payload sway responses with unshaped, ZV, ZVD and DZV shaped inputs for cable lengths of 0.326 m and 0.73 m respectively. The IAE values and maximum residual sway are summarised in Figures 23 and 24 respectively. The experiments verify the asymmetric robustness behavior of DZV shaper where highest robustness is shown for the case of 20% increase in the natural frequency, but less performance for the case of 20% decrease. Similar to the simulation results, ZV and ZVD shapers have the similar behavior for both +20% and -20% errors in natural frequency.
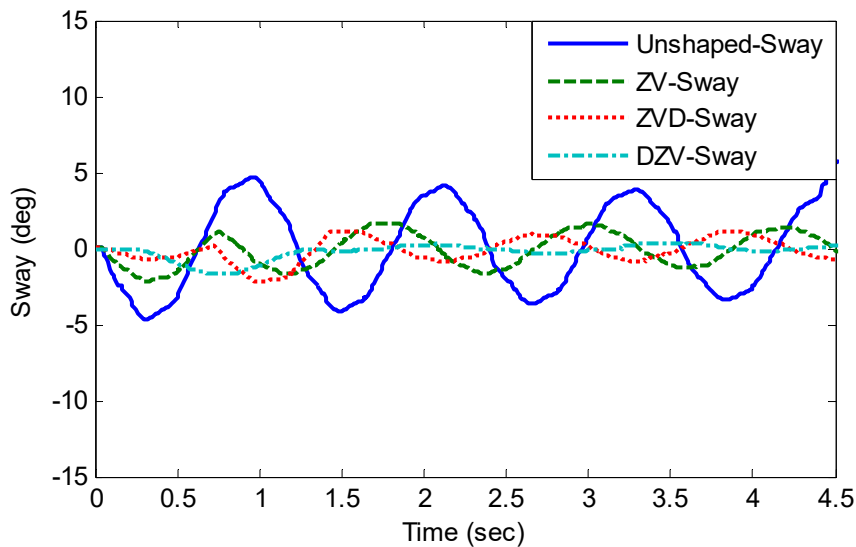

Figure 21: Payload sway with 20% increase in natural frequency (experiment)
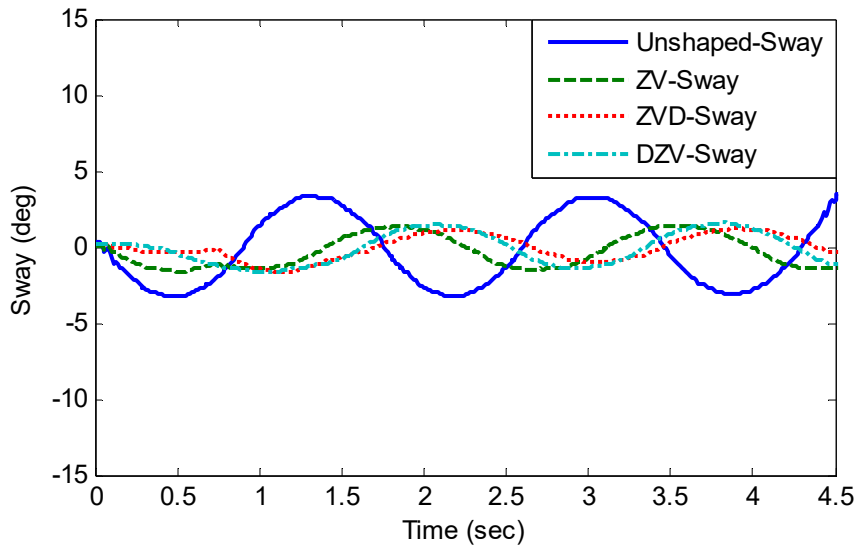
19

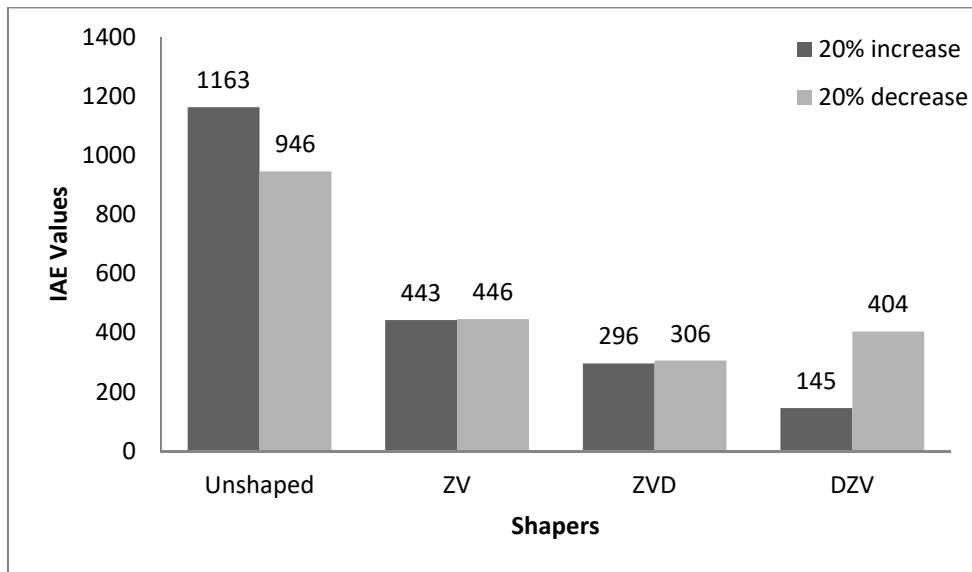Figure 22: Payload sway with 20% decrease in natural frequency (experiment)

Figure 23: IAE values of the payload sway for 20% increase and decrease in the natural frequency (experiment)
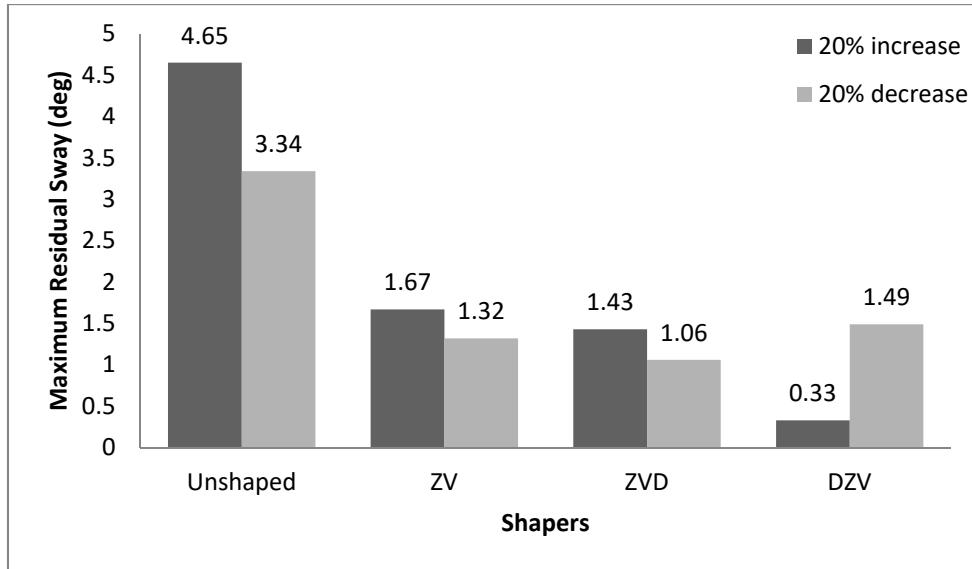
Figure 24: Maximum residual sway for 20% increase and 20% decrease in the natural frequency (experiment)

6. Conclusion

A new DZV shaper with ZV and ZVD shaping schemes have been designed and examined in reducing motion induced payload sway of a gantry crane in open-loop and closed-loop input shaping schemes. Simulation and experimental results have revealed that all the shapers are able to reduce payload sway significantly while maintaining desired position response specifications. Robustness tests with ±20% changes in the sway frequency (cable length changes) have shown that DZV shaper has an asymmetric robustness behavior. The shaper has highest robustness performance for 20% increase in the natural frequency (reduce cable length) but has the lowest robustness for the case of 20% decrease (increase cable length). ZV and ZVD show similar robustness performances in both cases. As more parameters are required for DZV shaper, it is also found that this shaper is difficult to be implemented as compared to ZV and ZVD shapers.

References

Abdel-Rahman EM, Nayfeh AH and Masoud ZN. (2003) Dynamics and control of cranes: A review. *Journal of Vibration and Control* 9(7): 863-908.

Butler H, Honderd G and Van Amerongen J. (1991) Model reference adaptive control of a gantry crane scale model. *IEEE Control Systems* 11(1): 57-62.

Crain EA, Singhose WE and Seering WP. (1996) Derivation and properties of convolved and simultaneous two-mode input shapers. *IFAC World Congress.* San Francisco, USA, 30 June – 5 July, pp. 441-446.

Gürleyük SS. (2011) Designing unity magnitude input shaping by using PWM technique. *Mechatronics* 21(1): 125-131.

Le TA, Lee S-G and Moon S-C. (2014) Partial feedback linearization and sliding mode techniques for 2D crane control. *Transactions of the Institute of Measurement and Control* 36(1): 78-87.

Mohamed Z, Martins JM, Tokhi MO, Sa da Costa J. and Botto MA. (2005) Vibration control of a very flexible manipulator system. *Control Engineering Practice* 13(3): 267-277.

Pao L and Singhose W. (1996) Unity magnitude input shapers and their relation to time-optimal control. *IFAC World Congress.* San Francisco, USA, 30 June – 5 July pp. 385-390.

Pauluk M, Korytowski A, Turnau A and Szymkat M. (2001) Time optimal control of 3D crane. *Proceedings of the 7th IEEE International Conference on Methods and Models in Automation and Robotics.* Międzyzdroje, Poland, 28-31 August, pp. 122-128.

Peng KCC, Singhose W and Frakes DH. (2012) Hand-Motion Crane Control Using Radio-Frequency Real-Time Location Systems. *IEEE/ASME Transactions on Mechatronics* 17(3): 464-471.

Pereira E, Trapero JR, Díaz IM, et al. (2012) Adaptive input shaping for single-link flexible manipulators using an algebraic identification. *Control Engineering Practice* 20(2): 138-147.

Singer N and Seering W. (1990) Preshaping command inputs to reduce system vibration. *ASME Journal of Dynamic Systems, Measurement, and Control* 112(1): 76-82.

Singer N, Singhose W and Kriikku E. (1997) An input shaping controller enabling cranes to move without sway. *ANS 7th Topical Meeting on Robotics and Remote Systems.* Georgia, USA, 27 April-1 May, pp. 225-231.

Singhose W. (2009) Command shaping for flexible systems: A review of the first 50 years. *International Journal of Precision Engineering and Manufacturing* 10(4): 153-168.

Singhose W, Derezinski S and Singer N. (1996) Extra-insensitive input shapers for controlling flexible spacecraft. *Journal of Guidance, Control, and Dynamics* 19(2): 385-391.

Singhose W, Singer N and Seering W. (1994) Design and implementation of time-optimal negative input shapers. *ASME Winter Annual Meeting.* Chicago, USA, 6-11 November, pp. 151-157.

Smith OJM. (1957) Posicast control of damped oscillatory systems. *Proceedings of the IRE* 45: 1249-1255.

Sorensen KL, Singhose W and Dickerson S. (2007) A controller enabling precise positioning and sway reduction in bridge and gantry cranes. *Control Engineering Practice* 15(7): 825-837.

Vyhlídal T, Kučera V and Hromčík M. (2013) Signal shaper with a distributed delay: Spectral analysis and design. *Automatica* 49(11): 3484-3489.

Yang M-J, Gu G-Y and Zhu L-M. (2014) High-bandwidth tracking control of piezo-actuated nanopositioning stages using closed-loop input shaper. *Mechatronics* 24(6): 724-733.

Yu X, Lin X and Lan W. (2014) Composite nonlinear feedback controller design for an overhead crane servo system. *Transactions of the Institute of Measurement and Control* 36(5): 662-672.